

UDC 541.6:548.737:543.422

DFT, FT-RAMAN, AND FT-IR INVESTIGATIONS OF 1-CYCLOPROPYLPIPERAZINE

G. Keşan¹, Ö. Alver², M. Bilge³, C. Parlak⁴¹Faculty of Science, University of South Bohemia, České Budějovice, Czech Republic²Department of Physics, Science Faculty, Anadolu University, Eskişehir, Turkey

E-mail: ozguralver@anadolu.edu.tr

³Department of Physics, Science Faculty, Ege University, İzmir, Turkey⁴Department of Physics, Dumlupınar University, Kütahya, Turkey

Received May, 12, 2012 г.

Revised — July, 12, 2013 г.

FT-IR and FT-Raman spectra of 1-cyclopropylpiperazine (1cPPP) are experimentally examined in the range 4000—200 cm⁻¹. The optimized geometric parameters, conformational equilibria, normal mode frequencies and corresponding vibrational assignments of 1cPPP C₇H₁₄N₂ are theoretically examined by means of B3LYP hybrid density functional theory (DFT) with the 6-31++G(d,p) basis set. Based on the potential energy distribution (PED) reliable vibrational assignments are made and the thermodynamics functions, highest occupied and lowest unoccupied molecular orbitals (HOMO and LUMO) of 1cPPP are predicted. Calculations are performed for four different conformations in two point groups of 1cPPP in the gas phase. A comparison between the experimental and theoretical results indicates that the B3LYP method is able to provide satisfactory results for the prediction of vibrational frequencies, structural parameters, and assignments. Furthermore, the C_s (equatorial-equatorial) point group is found as the most stable conformer of 1cPPP.

Keywords: 1-cyclopropylpiperazine, vibrational spectra, PED, DFT, B3LYP.

INTRODUCTION

Piperazine and its derivatives have an extensive range of applications in the field of materials science and organic synthesis. Many piperazine derivatives are of great interest in pharmacy and drugs. 1-cyclopropylpiperazine, known in the literature by synonyms such as N-cyclopropylpiperazine and 4-cyclopropylpiperazine, is a piperazine derivative. It has been used in the preparation of some tri- and tetrasubstituted ureas with histamine H₃ antagonist receptor activity [1], 3-amido-4-anilinoquinolines series as CSF-1R kinase inhibitors [2], for the synthesis of cyclopropyl amines as modulators of the histamine H₃ receptor [3], sulfonamide compounds as cysteine protease inhibitors [4], N-oxides as antibacterial agents [5] and in the treatment of the disease caused by helicobacter infection [6].

Vibrational spectroscopy has been extensively used for the structural characterization of molecular systems by DFT calculations [7—11]. Unlike Hartree-Fock theory, DFT includes electron correlation in the self-consistent Kohn-Sham procedure through the electron density functions, so it is a cost effective and reliable method [7—11]. The DFT/B3LYP model shows good performance on electron affinities, bond energies and reasonably good performance on vibrational frequencies and geometries of organic compounds [7—15].

Even though, 1cPPP has wide applications, to the best of our knowledge, there is no information present in literature about its spectroscopic properties. A detailed quantum chemical study is required to make definitive assignments to the fundamental normal modes of 1cPPP and to clarify the obtained experimental data for the title molecule. The detailed results of the theoretical and spectroscopic stu-

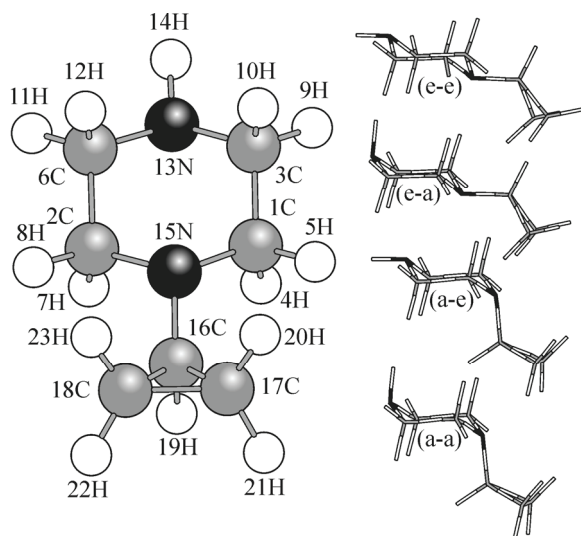


Fig. 1. Four different conformations in epy C_s point group and numbering of 1cPPP

dies are reported here. In the present study, we have reported the vibrational spectra of 1cPPP with PED data and the structural parameters of 1cPPP have also been calculated for the most stable conformer in the gas phase at the B3LYP/6-31++G(*d,p*) level.

EXPERIMENTAL

A commercial sample of N-cyclopropylpiperazine was purchased (Santa Cruz Biotechnology, $\geq 98\%$) and used without further purification. FT-MIR and FT-FIR spectra of 1cPPP were recorded in the range $4000\text{--}200\text{ cm}^{-1}$ with a Bruker Optics IFS66v/s FTIR spectrometer with the resolution of 2 cm^{-1} .

The FT-Raman spectrum was obtained using a Bruker Senterra Dispersive Raman microscope spectrometer with 532 nm excitation from a 3B diode laser having 3 cm^{-1} resolution in the spectral range $4000\text{--}200\text{ cm}^{-1}$.

CALCULATIONS

Calculations were performed using the Gaussian 09.A1 program [16] on a personal computer and GaussView 5.0.8 [17] was used for the visualization of the structure and simulated vibrational spectra. Many possible conformers could be suggested for 1cPPP (Fig. 1), but most of them are energetically not possible, so the investigation was limited to e-e (equatorial-equatorial), e-a (equatorial-axial), a-a (axial-axial), and a-e (axial-equatorial) conformers in both C_s and C_1 point groups of the title molecule and where the former represents NH while the latter stands for the cyclopropane group (Fig. 1).

They are considered in axial and equatorial positions according to the plane formed by C1, C2, C3 and C6 carbon atoms of 1cPPP. For the calculations, all four forms of 1cPPP were first optimized by B3LYP with the 6-31++G(*d,p*) basis set in the gas phase. The e-e conformation belonging to the C_s point group (e-e (C_s)) was found to be more stable than the other forms (Table 1).

Table 1

Point groups, conformers, gibbs free energy, relative stability and mole fractions of 1cPPP by B3LYP with 6-31++G(*d,p*) basis set

Point group	Conformers	ΔG (Hartree)	Relative stability ^a ($\delta\Delta G$, kcal/mol)	Mole fractions (%)
C_s	e-e	-384.485062	0.000	0.27
	e-a	-384.484347	0.449	0.24
	a-e	-384.479428	3.535	—
	a-a	-384.478329	4.225	—
C_1	e-e	-384.484954	0.068	0.26
	e-a	-384.484345	0.450	0.23
	a-e	-384.479377	3.567	—
	a-a	-384.478171	4.324	—

^a Relative stability were calculated compared to C_s (e-e) conformer.

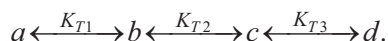
Therefore, for the vibrational calculations, the vibrational frequencies of the e-e(C_s) conformer of 1cPPP were calculated using the same method and basis set under the keyword freq = Raman, pop = full and then scaled by 0.955 (above 1800 cm^{-1}) and 0.977 (under 1800 cm^{-1}) for 6-31++G(d,p) [13, 14]. The polarizable continuum model [18], which is the default in Gaussian 09.A1, was used for the geometries, free energies, and vibrational frequencies. The absence of imaginary frequencies confirmed that the optimization was successfully performed.

PED calculations; which indicate the relative contributions of the redundant internal coordinates to each normal vibrational mode of the molecule and thus make it possible to identify the character of each mode numerically; were carried out by the VEDA 4 (Vibrational Energy Distribution Analysis) [19] program. The VEDA program does not scale the elements of the force constant matrix as proposed by Pulay *et al.* [20]. For details of the PED analysis for the VEDA program, more information was published in [21].

RESULTS AND DISCUSSION

The results of the calculations on the molecular conformations and geometrical parameters of 1cPPP are discussed first. A brief discussion of the experimental and theoretical vibrational frequencies and intensities is then presented.

Geometrical structures. Gibbs free energies, relative stabilities, and molar fractions of the optimized geometries in the gas phase of four conformations in two point groups of 1cPPP calculated with DFT/6-31++G(d,p) are given in Table 1. Regarding the relative stability energies given in Table 1, the molar fractions of a-e(C_s), a-a(C_s), a-e(C_1), and a-a(C_1) conformers could be ignored since their relative stabilities compared to the e-e(C_s) conformer are more than 2.0 kcal/mol. The molar fractions for individual e-e(C_s), e-e(C_1), e-a(C_s), and e-a(C_1) conformers, where a , b , c and d respectively, can be calculated with the following equations:



According to the equilibrium given above,

$$K_{T1} = N_b/N_a, \quad K_{T2} = N_c/N_b, \quad K_{T3} = N_d/N_c$$

and

$$N_a + N_b + N_c + N_d = 1$$

can be written, where K_{T1} , K_{T2} and K_{T3} are the conformational equilibrium constants between a , b , c and d forms, N_a , N_b , N_c and N_d are the molar fractions of conformers a , b , c and d .

$$N_a = \frac{1}{1 + K_{T1} + K_{T1}K_{T2} + K_{T1}K_{T2}K_{T3}},$$

$$N_b = \frac{K_{T1}}{1 + K_{T1} + K_{T1}K_{T2} + K_{T1}K_{T2}K_{T3}},$$

$$N_c = \frac{K_{T1}K_{T2}}{1 + K_{T1} + K_{T1}K_{T2} + K_{T1}K_{T2}K_{T3}},$$

$$N_d = \frac{K_{T1}K_{T2}K_{T3}}{1 + K_{T1} + K_{T1}K_{T2} + K_{T1}K_{T2}K_{T3}}.$$

$K_T = e^{-\Delta G/RT}$, $R = 1.987 \times 10^{-3}$ kcal/mol·K, $T = 298$ K and $\delta\Delta G = \Delta G_b - \Delta G_a$ [22].

Regarding the calculated free energies for the gas phase, the following molar fractions were obtained: $N_a = 0.27$ (e-e(C_s)), $N_b = 0.26$ (e-e(C_1)), $N_c = 0.24$ (e-a(C_s)), and $N_d = 0.23$ (e-a(C_1)). Based on the calculations, the e-e(C_s) form is most stable and the most abundant conformer in the gas phase. Since N_a is larger than N_b , N_c , and N_d , the approximate mode descriptions were determined considering the e-e(C_s) conformer.

Some optimized geometric parameters (bond lengths, bond and dihedral angles) calculated by B3LYP/6-31++G(d,p) are listed in Table 2. To the best of our knowledge, the experimental data on the geometric structure of 1cPPP is not available in the literature. Therefore, the theoretical results

Table 2

Optimized geometric parameters for four conformers of 1cPPP in gas phase

Parameter	Experi- mental ^{a,b}	B3LYP/6-31++G(d,p)			
		C ₁		C _s	
		e-e	e-a	e-e	e-a
Bond Lengths, Å					
N13—H14		1.02	1.02	1.02	1.02
(C—N)pp	1.47 ^a	1.47	1.47	1.47	1.47
(C—C)pp	1.54 ^a	1.53	1.54	1.53	1.54
(C—H)pp	1.11 ^a	1.10	1.10	1.10	1.10
(C—C)cp	1.51 ^b	1.51	1.51	1.51	1.51
(C—H)cp	1.08 ^b	1.09	1.09	1.09	1.09
C16—N15		1.44	1.44	1.44	1.43
Bond Angles, deg.					
(C—C—N)pp	110.4 ^a	109.8	112.2	109.8	111.1
(C—N—C)pp	109.0 ^a	111.2	111.1	111.2	111.1
(H—C—H)pp	109.1 ^a	108.1	107.7	108.1	107.5
(H—C—H)cp	115.9 ^b	115.1	115.0	115.0	115.0
C17—C16—H19		116.3	116.4	116.3	116.4
C18—C16—H19		116.3	116.4	116.3	116.4
C17—C16—N15		118.4	118.4	118.3	118.4
C18—C16—N15		118.4	118.4	118.3	118.4
C1—N15—C16		112.3	112.4	112.4	112.4
C2—N15—C16		112.3	112.4	112.4	112.4
N15—C16—H19		115.8	115.7	115.9	115.7
Dihedral Angles, deg.					
C1—C3—N13—H14		-176.1	-70.6	-174.0	-70.6
C2—C6—N13—H14		176.1	70.6	177.0	70.6
C6—C2—N15—C16		176.0	175.9	174.7	175.9
C3—C1—N15—C16		-176.0	-175.9	-175.7	-175.9
C1—N15—C16—C17		82.2	82.1	82.1	82.1
C1—N15—C16—C18		151.8	151.7	151.6	151.7
C2—N15—C16—C17		-151.8	-151.7	-151.6	-151.7
C2—N15—C16—C18		-82.2	-82.0	-82.1	-82.1
C1—N15—C16—H19		-63.0	-63.1	-63.1	-63.1
C2—N15—C16—H19		63.0	63.1	63.1	63.1

^{a,b} Taken from [23, 24], respectively. pp, piperazine; cp, cyclopropane.

have been compared with the experimental data for piperazine [23] and cyclopropane [24] compounds as given in Table 2. The magnitude of dihedral angles for the optimized 1cPPP (the D(2;6;13;14) angles) are found to be 177° in e-e(C_s) and e-e(C₁) conformers and also 71° in e-a(C₁) and e-a(C_s). Moreover, the D(15;16;2;6) angles are found as 176° in e-e(C₁) and e-a(C₁), 175° in e-e(C_s) and e-a(C_s).

Several thermodynamic parameters, capacity, zero point energy, entropy etc., calculated by the DFT/B3LYP/6-31++G(d,p) method are presented in Table 3. The variation in the zero point vibra-

Table 3

Thermodynamic parameters for four conformers of 1cPPP in gas phase

Parameter	B3LYP/6-31++G(d,p)			
	C_1		C_s	
	e-e	e-a	e-e	e-a
Thermal total energy, kcal/mol	136.628	136.571	136.604	136.571
Vibrational energy, kcal/mol	134.850	134.793	134.826	134.793
Zero point vibrational energy, kcal/mol	131.366	131.292	131.330	131.292
Dipole moment, D	0.506	1.489	0.505	1.489
Heat capacity, kcal/mol·K	0.335	0.336	0.335	0.336
Entropy, kcal/mol·K	0.890	0.891	0.891	0.891

tional energy seems to be insignificant. The total energy and change in the entropy of 1cPPP are calculated at room temperature.

VIBRATIONAL STUDIES OF 1CPPP

To the best of our knowledge, the vibrational frequencies and assignments of 1cPPP in the range 4000—200 cm^{-1} have not been reported in the literature. The measured and calculated vibrational frequencies along with the corresponding vibrational assignments and intensities and the theoretical-experimental vibrational spectra of 1cPPP are given in Table 4 and Figs. 2 and 3 respectively.

The 1cPPP molecule consists of 23 atoms, so it has 63 normal vibrational modes and its most stable form belongs to the point group C_s with the only identity (E) symmetry element or operation. The assignments of vibrational modes of 1cPPP in the e-e form have been provided by VEDA 4 [19] in Tables 4. According to the calculations, 3 normal vibrational modes of 1cPPP are below 200 cm^{-1} .

The high wavenumber region contains a characteristic NH stretching band of 1cPPP attributed to the piperazine group. Free piperazine has a main NH band at 3225 cm^{-1} in the IR spectrum [25]. The strong broad NH stretching in the title molecule is assigned to 3275 cm^{-1} in the IR spectrum and 3353 cm^{-1} in the Raman spectrum. The corresponding scaled theoretical values of these modes are 3380 cm^{-1} with 0.955 and 3353 cm^{-1} with SQM methodology with a 100 % PED contribution. The asymmetric and symmetric CH_2 vibrations in 1cPPP arise from both piperazine and cyclopropyl groups. The vibrational bands at 3085 cm^{-1} , 3006 cm^{-1} in the IR spectrum and 3084 cm^{-1} , 3073 cm^{-1} , 3008 cm^{-1} , 2986 cm^{-1} in the Raman spectrum are due to symmetric and antisymmetric CH_2 vibrations arising from the cyclopropyl group. The corresponding scaled calculated values for these bands were found as between (3087—2997) cm^{-1} with 0.955 and (3087—2996) cm^{-1} with SQM methodology. For the title molecule the CH_2 stretching bands in piperazine have been observed at 2939 cm^{-1} , 2910 cm^{-1} , 2812 cm^{-1} in the IR spectrum and 2945 cm^{-1} , 2929 cm^{-1} , 2847 cm^{-1} , 2806 cm^{-1} in the Raman spectrum, while the present theoretical findings are between (2944—2812) cm^{-1} with 0.955 and (2943—2812) cm^{-1} with SQM methodology. In the high wavenumber region of the spectra, the anharmonicity can explain differences between the experimental and calculated values. Additionally, these differences can be due to the intra- and intermolecular hydrogen bondings or a laser used for Raman.

The fundamental CH_2 vibrations, which are scissoring, twisting, wagging, and rocking, appear in the expected frequency region 1600—800 cm^{-1} [26]. These vibrations were revealed to be mixed CH_2 wagging, CH_2 twisting, CH_2 rocking, CH_2 scissoring, CNH bending, CC or CN stretching. Experimental/calculated (0.977, SQM) $\delta(\text{CH}_2)$ scissoring modes arising from both piperazine and cyclopropyl groups are found as 1453/1454 (0.977, SQM) cm^{-1} in the IR spectrum and 1455/1459 (0.977, SQM) cm^{-1} , 1477/1472 (0.977) cm^{-1} , 1475 (SQM) cm^{-1} in the Raman spectrum. The bands appeared at 1440 (R) cm^{-1} , 1416 (IR, R) cm^{-1} , 1383 (IR) cm^{-1} are mainly due to CNH bending vibrations calculated as (1447—1383) cm^{-1} with 0.977 and (1442—1381) cm^{-1} with SQM methodology. Based on the PED assignments, the bands at 1362 cm^{-1} in both IR and Raman spectra mainly arise from the mixed

Table 4

Comparison of the experimental and calculated vibrational wavenumbers (cm^{-1}) of 1cphp in gas phase

Mode	Assignment PED ($\geq 5\%$)	Experimental		B3LYP/6-31++G(d,p) e-e (C_s) in gas phase				
		IR	Raman	ν^α	ν^β	ν^ϕ	I_{IR}	I_{R}
ν_1	v(NH) 100	3275 s	3353 wb	3539	3380	3353	0.01	24.52
ν_2	v(CH) 100	3085 s	3084 m	3233	3087	3087	20.37	7.93
ν_3	v(CH) 100	—	3073 m	3220	3075	3075	0.30	14.86
ν_4	v(CH) 99	3006 s	3008 vs	3142	3001	3000	9.49	41.80
ν_5	v(CH) 100	—	2986 s	3138	2997	2996	21.42	8.03
ν_6	v(CH) 94	2939 vs	—	3083	2944	2943	59.91	4.30
ν_7	v(CH) 90	—	2945 s	3076	2938	2937	42.74	17.86
ν_8	v(CH) 93	2910 vs	2929 m	3076	2937	2937	35.29	26.48
ν_9	v(CH) 99	—	2847 m	3028	2891	2891	75.28	27.40
ν_{10}	v(CH) 95	2812 vs	2806 m	2945	2812	2812	234.32	11.41
ν_{11}	$\delta(\text{HCH})$ 89	—	1477 m	1507	1472	1475	1.61	7.82
ν_{12}	$\delta(\text{HCH})$ 91	1453 vs	1455 m	1489	1454	1459	0.16	13.00
ν_{13}	$\delta(\text{HCN})$ 82	—	1440 m	1481	1447	1442	3.25	1.06
ν_{14}	$\delta(\text{HCN})$ 64	1416 m	1416 m	1432	1399	1398	3.92	2.51
ν_{15}	$\delta(\text{HCN})$ 62	1383 m	—	1415	1383	1381	1.06	0.82
ν_{16}	$\delta(\text{HCN})$ 57 + $\nu(\text{NC})$ 17	1362 vs	1362 m	1397	1365	1364	56.04	2.53
ν_{17}	$\delta(\text{HCC})$ 73	1339 s	1322 w	1371	1340	1337	15.81	0.57
ν_{18}	$\delta(\text{HCC})$ 61	1317 s	1301 m	1350	1319	1315	26.94	1.32
ν_{19}	$\delta(\text{HCN})$ 76	—	1295 vw	1329	1299	1295	1.96	11.70
ν_{20}	$\delta(\text{HCN})$ 74	1264 vs	—	1299	1269	1267	10.56	1.04
ν_{21}	$\delta(\text{HCC})$ 54 + $\nu(\text{NC})$ 15	1251 s	—	1277	1247	1243	15.19	0.14
ν_{22}	$\nu(\text{NC})$ 57 + $\delta(\text{HCH})$ 10 + $\delta(\text{HCN})$ 10	1214 vs	1213 vs	1244	1215	1213	22.45	17.94
ν_{23}	$\delta(\text{HCN})$ 85	—	1201 m	1220	1192	1191	0.02	7.79
ν_{24}	$\nu(\text{CC})$ 37 + $\delta(\text{HCC})$ 13	1183 s	1187 m	1207	1180	1179	10.27	5.77
ν_{25}	$\delta(\text{HCC})$ 81	—	1166 w	1195	1168	1169	0.87	1.93
ν_{26}	$\nu(\text{NC})$ 52 + $\delta(\text{HCC})$ 16	—	1151 w	1169	1142	1140	0.04	5.23
ν_{27}	$\nu(\text{NC})$ 75	1140 vs	1133 m	1162	1135	1135	50.10	0.30
ν_{28}	$\tau(\text{HCNC})$ 57	1125 s	—	1140	1113	1125	0.55	4.14
ν_{29}	$\tau(\text{HCNC})$ 68	—	1105 w	1132	1106	1100	0.46	1.07
ν_{30}	$\delta(\text{HCC})$ 81	1063 s	1057 m	1081	1056	1056	0.37	0.08
ν_{31}	$\tau(\text{HCCC})$ 83	1016 vs	1019 w	1050	1026	1021	14.66	1.53
ν_{32}	$\nu(\text{CC})$ 17 + $\nu(\text{NC})$ 42 + $\delta(\text{HCC})$ 11	990 s	984 m	1006	982	983	6.71	4.19
ν_{33}	$\nu(\text{CC})$ 51 + $\tau(\text{HCCC})$ 17	967 m	963 vw	984	961	958	2.52	2.40
ν_{34}	$\nu(\text{NC})$ 77	899 s	896 m	915	893	893	20.09	5.03
ν_{35}	$\nu(\text{CC})$ 71	860 vs	870 m	908	887	884	0.25	2.89
ν_{36}	$\nu(\text{NC})$ 13 + $\delta(\text{HCC})$ 48	—	843 s	867	847	847	0.35	0.83
ν_{37}	$\nu(\text{CC})$ 76	—	824 m	864	845	845	7.56	15.33
ν_{38}	$\tau(\text{HCCC})$ 59+ $\tau(\text{HCNC})$ 10+ $\nu(\text{CC})$ 23	822 vs	809 m	835	816	810	8.41	4.09
ν_{39}	$\nu(\text{NC})$ 14 + $\delta(\text{HCC})$ 35	777 vs	793 m	803	785	783	24.76	3.19
ν_{40}	$\delta(\text{HCC})$ 48 + $\nu(\text{CC})$ 13	747 s	747 m	754	737	736	4.99	6.84

Continued Table 1

1	2	3	4	5	6	7	8	9
ν_{41}	$\delta(\text{HNC})$ 65	565 s	544 w	562	549	546	35.65	7.14
ν_{42}	$\tau(\text{HCNH})$ 66	490 w	481 m	483	472	470	0.01	8.73
ν_{43}	$\tau(\text{HCCN})$ 54 + $\tau(\text{HCNC})$ 10	467 w	444 m	464	453	454	1.96	9.39
ν_{44}	$\tau(\text{HCNC})$ 63	422 vw	400 w	420	410	416	2.96	10.07
ν_{45}	$\tau(\text{HCNC})$ 52	352 vs	324 w	347	339	340	3.30	15.84
ν_{46}	$\tau(\text{HCCN})$ 79	—	297 w	269	263	269	0.86	0.52
ν_{47}	$\tau(\text{HCNC})$ 75	274 vs	268 w	263	257	261	4.88	1.56

Note: ν^a : Unscaled wavenumbers. ν^b : scaled with 0.955 above 1800 cm^{-1} , 0.977 under 1800 cm^{-1} . ν^c : scaled by SQM methodology. I_{IR} and I_{R} : Calculated infrared and Raman intensities. PED data are taken from VEDA4. v: very, s: strong, m: medium, w: weak, b: broad.

type combination of CN(15) stretching and HCN(15) bending, which are theoretically calculated at 1365 cm^{-1} with 0.977 and 1364 cm^{-1} with SQM. The NC stretching in the piperazine ring is 1140 cm^{-1} in the IR spectrum, 1133 cm^{-1} in the Raman spectrum, while the present theoretical findings is 1135 cm^{-1} with both 0.977 and SQM methodology with a 75 % PED contribution. Moreover, the NC

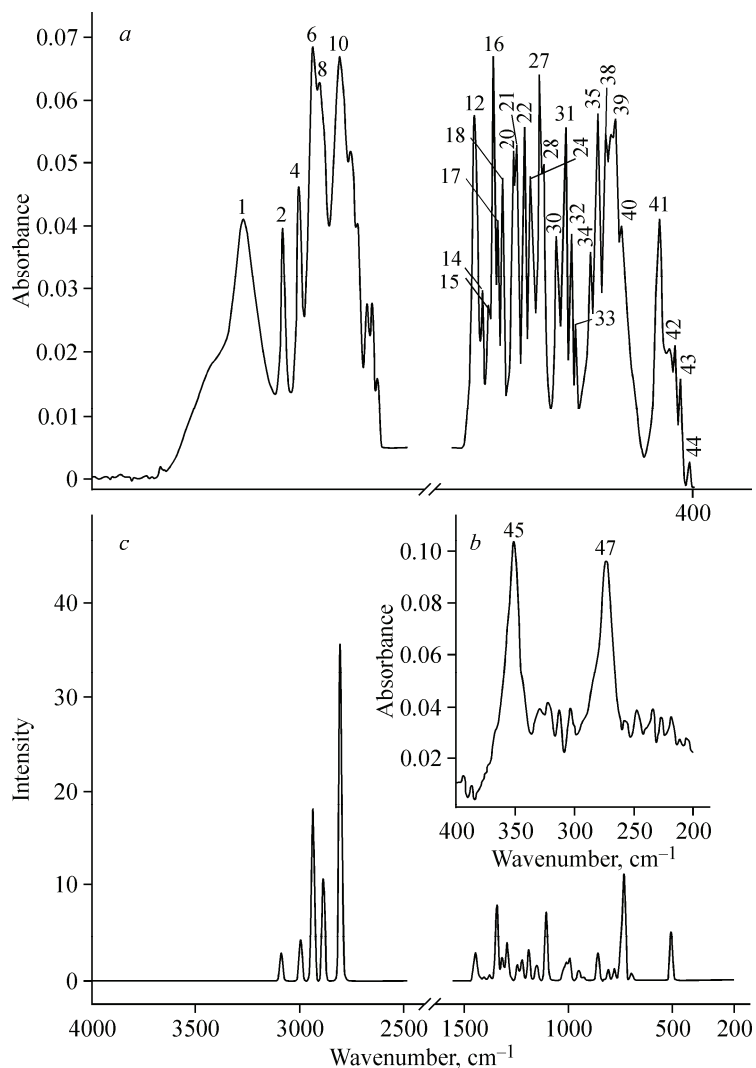


Fig. 2. Experimental (*a* and *b*) and scaled calculated (*c*) IR spectra of 1c ppp

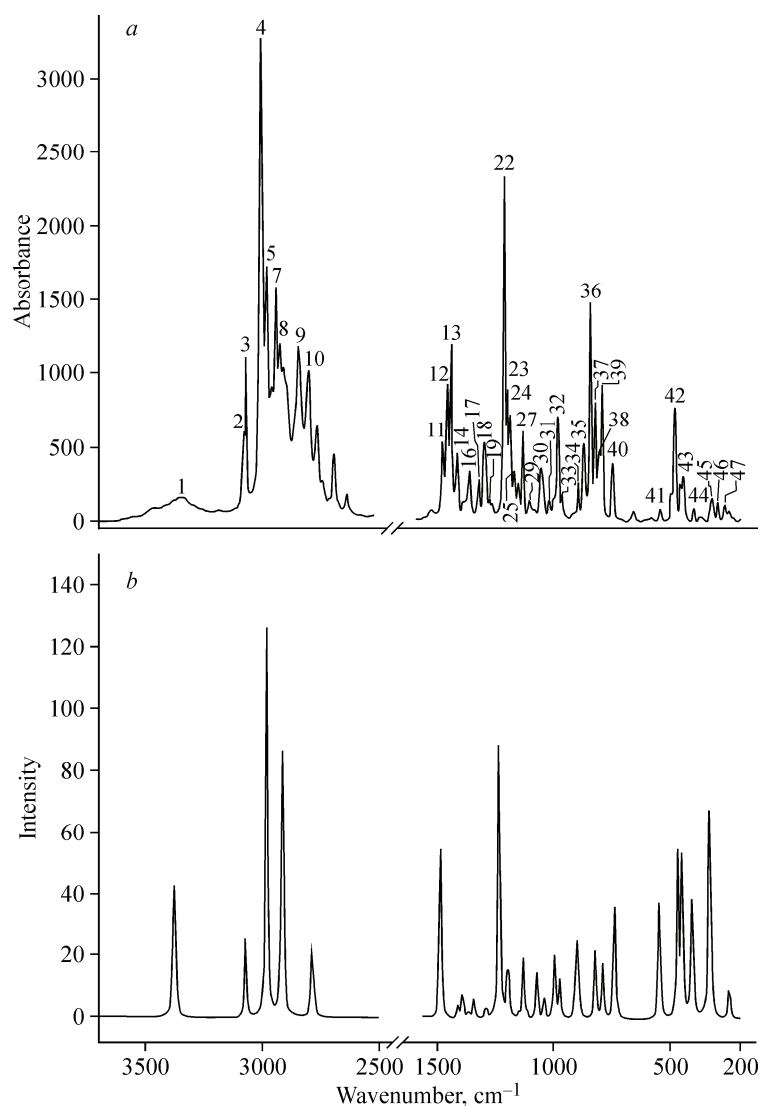


Fig. 3. Experimental (a) and scaled calculated (b) Raman spectra of 1cppp

and CC stretching modes, which arise from both piperazine and cyclopropyl groups, are also observed at 899 cm^{-1} , 860 cm^{-1} in the IR spectrum and 896 cm^{-1} , 870 cm^{-1} in the Raman spectrum. The corresponding scaled theoretical values of these modes are 893 cm^{-1} , 887 cm^{-1} with 0.977 and 893 cm^{-1} , 894 cm^{-1} with SQM methodology.

CC or CN stretching, CCC or CCH bending, and some torsion modes dominate the region of $1000\text{--}500\text{ cm}^{-1}$, while CCC or CCN bending and CCCN, CCNH, CCCH or CCCC torsion modes are seen in the low-frequency region. Similar situations have been shown for the calculations. Vibrational modes in the low wavenumber region of the spectrum contain contributions of several internal coordinates and their assignments have a reduction approximation to one of two of the internal coordinates.

It can be drawn from Tables 4 and Figs. 2 and 3 that there is good agreement between the experimental and theoretical vibrational frequencies. In order to compare the experimental frequencies, we have found the correlation graphics based on the calculations (Fig. 4).

The correlation values between the experimental and calculated vibrational frequencies are found to be 0.9996 (IR) and 0.9997 (R) with 0.955–0.977 and 0.9998 (IR) and 0.9997 (R) with SQM.

It can be seen that the B3LYP/6-31++G(*d,p*) calculation is reliable for the vibrational spectra.

Calculated Raman activities are converted to relative Raman intensities using the following relationship derived from the intensity theory of Raman scattering:

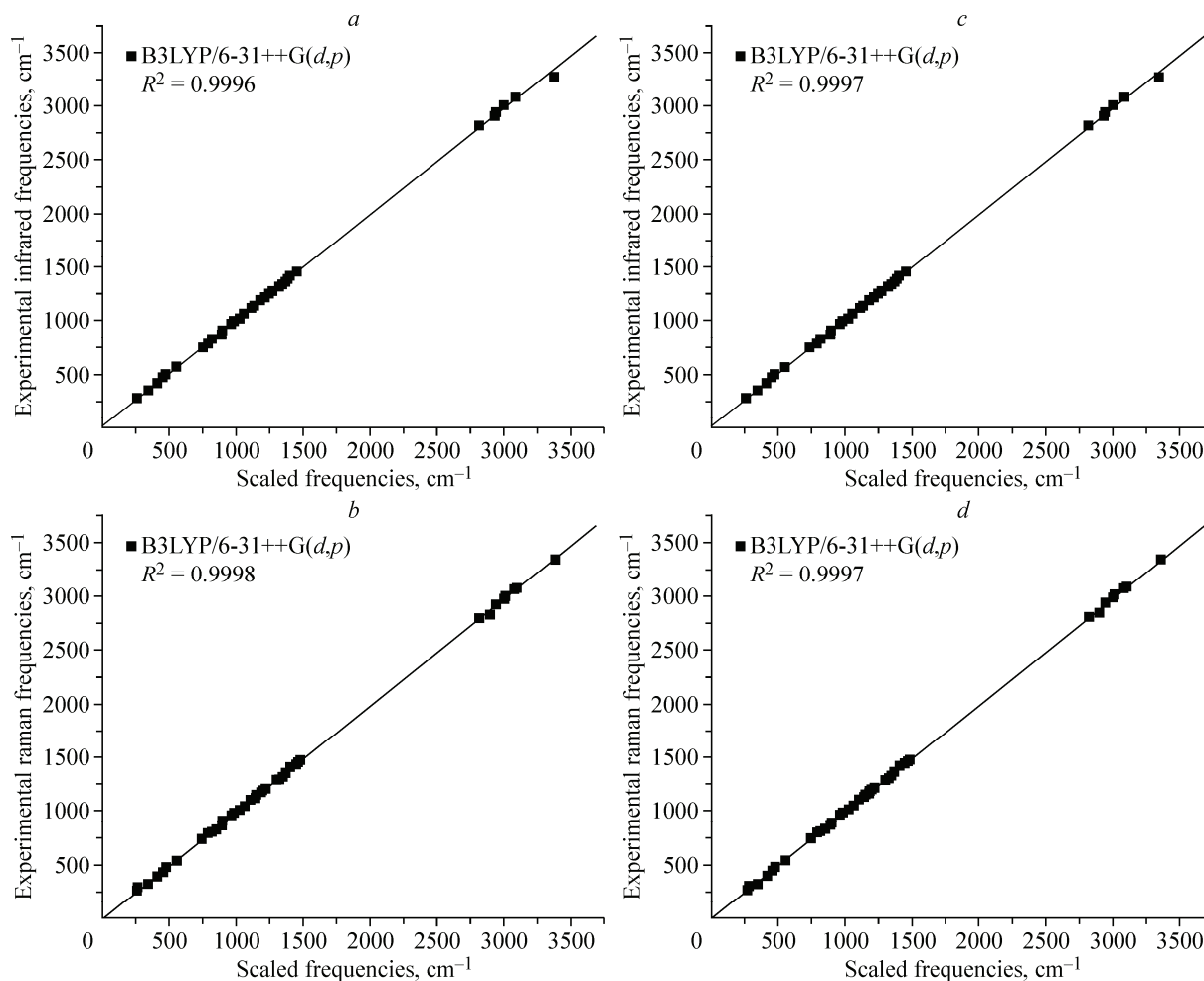


Fig. 4. Correlation graphics between the experimental and scaled calculated frequencies for 1cPPP

$$I_i = f(\nu_0 - \nu_i)^4 S_i / \nu_i [1 - \exp(-h\nu_i / kT)],$$

where ν_0 is the laser exciting wavenumbers in cm⁻¹, ν_i is the vibrational wavenumbers of the *i*th normal mode, S_i is the Raman scattering activity of the normal mode ν_i , and f is a suitably chosen common normalization factor for all peak intensities, 10⁻¹⁴. h , k , c and T are the Planck and Boltzmann constants, speed of light, and temperature in Kelvin respectively [15, 27].

The HOMO and LUMO orbitals are the main orbitals taking part in chemical stability. HOMO describes the ability to donate an electron and LUMO as an electron acceptor. The electronic transition absorption is defined from the ground to the first excited state. In other words, the transitions can be described from HOMO to LUMO. HOMO is located over all carbon and N15 atoms in 1cPPP, while LUMO is dominant for the N13 atom. The atomic compositions of the frontier molecular orbital and their orbital energies are shown in Fig. 5.

CONCLUSIONS

We performed the experimental and theoretical vibrational analysis of 1cPPP for the first time. FT-IR and FT-Raman spectra have been recorded in the range 4000–200 cm⁻¹. Some important vibrational bands have been discussed and assigned based on the calculated IR intensities and Raman activities. The structural parameters, IR and Raman frequencies, and intensities-activities of the vibrational bands of 1cPPP were calculated with density functional theory and the 6-31++G(*d,p*) basis set for C1 and C_s conformers. The e-e (C_s) conformation was found to be more stable than the other eight

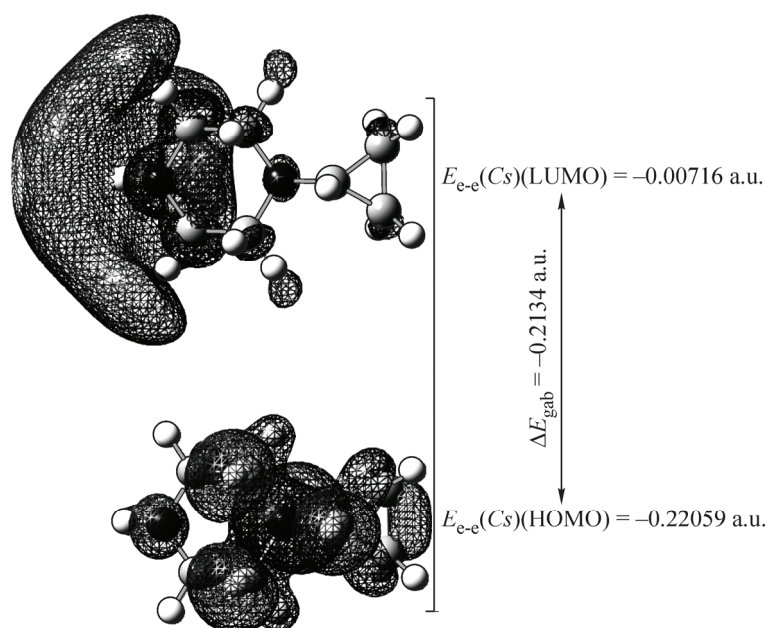


Fig. 5. Atomic orbital compositions of the frontier molecular orbital for 1cPPP

forms. In order to make a comparison with the experimental wavenumbers, we calculated the root mean square deviation (RMSD) based on the calculation. The following rmsd values were obtained: 21.26 cm^{-1} (IR, 0.955/0.977), 17.19 cm^{-1} (IR, SQM) and 12.97 cm^{-1} (R, 0.955/0.977), 11.81 cm^{-1} (R, SQM). The gas phase energy calculations and the obtained experimental-theoretical rmsd results indicate that it is the most stable conformer of the 1cPPP molecule. Any differences observed between the experimental and calculated wavenumbers could be due to the fact that the calculated ones have been obtained for a single molecule in the gaseous state contrary to the experimental values recorded in the presence of intermolecular interactions and increasing tendency to unharmonic vibrations in the high wavenumber region. Henceforth, the assignments made at the B3LYP/6-31++G(*d,p*) level of theory with only reasonable deviations from the experimental values seem feasible.

Acknowledgements. We are deeply grateful to M. Fatih KAYA for the VEDA 4 program.

REFERENCES

1. Lau J.F., Jeppesen C.B., Rinvall K., Hohlweg R. // *Bioorg. Med. Chem. Lett.* – 2006. – **16**. – P. 5303 – 5308.
2. Scott D.A., Bell K.J., Campbell C.T., Cook D.J., Dakin L.A., Del Valle D.J., Drew L., Gero T.W., Hattersley M.M., Omer C.A., Tyurin B., Zheng X. // *Bioorg. Med. Chem. Lett.* – 2009. – **19**. – P. 701 – 705.
3. Allison B.D., Carruthers N.I., Grice C.A., Letavic M.A. US Patent, No. 0066821 A1, 2007.
4. Woo S.H., Vivian R.W., Link J.O. US Patent, No. 0233909 A1, 2009.
5. Rast H., Scheer M., Hallenbach W. US Patent, No. 6114351, 2000.
6. Yamashita K., Yamane T., Sakashita S., Fujii K., Saka Y. US Patent, No. 5981522, 1999.
7. Scott A.P., Radom L. // *J. Phys. Chem.* – 1996. – **100**. – P. 16502 – 16513.
8. Ocola E.J., Brito T., McCann K., Laane J. // *J. Mol. Struct.* – 2010. – **978**. – P. 74 – 78.
9. Breda S., Reva I., Fausto R. // *J. Mol. Struct.* – 2008. – **887**. – P. 75 – 86.
10. Durig J.R., Ganguly A., El Defrawy A.M., Guirgis G.A., Gounev T.K., Herrebout W.A., Van Der Veken B.J. // *J. Mol. Struct.* – 2009. – **918**. – P. 64 – 76.
11. Yavuz M., Tanak H. // *J. Mol. Struct.: THEOCHEM.* – 2010. – **961**, N 1-3. – P. 9 – 16.
12. Parlak C. // *J. Mol. Struct.* – 2010. – **966**. – P. 1 – 7.
13. Alver Ö., Parlak C. // *J. Mol. Struct.* – 2010. – **975**. – P. 85 – 92.
14. Alver Ö., Parlak C. // *J. Theor. Comput. Chem.* – 2010. – **9**. – P. 667 – 685.
15. Alver Ö., Parlak C. // *Vib. Spectrosc.* – 2010. – **54**. – P. 1 – 9.

16. *Frisch M.J., Trucks G.W., Schlegel H.B. et al.* Gaussian 09, Revision A.1, Gaussian Inc., Wallingford, CT, 2009.
17. *Dennington R.D., Keith T.A., Millam J.M.* GaussView, Version 5.0.8, Gaussian Inc., Wallingford, CT, 2008.
18. *Miertus S., Scrocco E., Tomasi J.* // *Chem. Phys.* – 1981. – **55**. – P. 117 – 129.
19. *Jamróz M.H.* Vibrational energy distribution analysis: VEDA 4 program, Warsaw, 2004.
20. *Pulay P., Forgasi G., Pongor G., Boggs J.E., Vargha A.* // *J. Amer. Chem. Soc.* – 1983. – **105**. – P. 7037 – 7047.
21. *Jamróz M.H., Dobrowolski J.Cz., Brzozowski R.* // *J. Mol. Struct.* – 2006. – **787**. – P. 172 – 183.
22. *Hür D., Güven A.* // *J. Mol. Struct. (Theochem.)*. – 2002. – **583**. – P. 1 – 18.
23. *Yokazeki A., Kuchitsu K.* // *Bull. Chem. Soc. Jpn.* – 1971. – **44**. – P. 2352 – 2355.
24. *Gauss J., Cremer D., Stanton J.F.* // *J. Phys. Chem. A.* – 2000. – **104**. – P. 1319 – 1324.
25. *Hendra P.J., Powell D.B.* // *Spectrochim. Acta.* – 1962. – **18**. – P. 299 – 306.
26. *Vedal D., Ellestad O.H., Klaboe P., Hagen G.* // *Spectrochim. Acta A.* – 1976. – **32**. – P. 877 – 890.
27. *Keresztury G., Holly S., Varga J., Besenyi G., Wang A.Y., Durig J.R.* // *Spectrochim. Acta A.* – 1993. – **49**. – P. 2007 – 2026.